

Design and fabrication of modular supercapacitors using 3D printing

Anan Tanwilaisiri*, Yanmeng Xu, Ruirong Zhang, David Harrison, John Fyson, Milad Areir

College of Engineering, Design and Physical Sciences Brunel University London, UK

ARTICLE INFO

Article history:

Received 6 September 2017

Received in revised form 8 November 2017

Accepted 29 December 2017

Available online xxx

Keywords:

3D printing

Supercapacitors

Fused deposition modeling printing

Paste extrusion system

Energy storage device

ABSTRACT

Development in multi-material freeform 3D fabrication processes can provide the possibility of building complete functional electronic devices. This paper describes a design and manufacturing process for electrochemical supercapacitors. A combination of two 3D printing systems, i.e. a Fused Deposition Modelling (FDM) printer and a paste extruder, were applied to fabricate these energy storage devices. During the manufacturing process of supercapacitor components, the FDM 3D printer was used to print the packaging frames, the conductive layers, and the electrodes layers; and the separator with electrolyte were deposited using the paste extruder. Several complete energy storage supercapacitors have been made and their electrochemical performances were assessed. The 3D manufacturing process developed was also evaluated in this study.

© 2017 Elsevier Ltd. All rights reserved.

1. Introduction

Additive manufacturing (AM) (mostly referred to as 3D printing) is a method of manufacturing in which a model designed by Computer Aided Design (CAD) is captured and then consequently constructed on a layer by layer basis. 3D printing is considered as a promising tool for rapid production of 3D objects. At present, the technologies of additive manufacturing are becoming increasingly capable and affordable [1–3]. Current research focuses on the development of novel materials and the improvement of new techniques in order to fabricate a wide range of applications for many purposes. Improvement in 3D printing techniques enhanced with component placement and electrical interconnect deposition can offer the ability to make electronic prototypes. These developments provide integration of electronic components with 3D printed devices. This type of 3D electronics integration is also identified as 3D structural electronics or 3D printed electronics. 3D printed electronics can be designed to any form providing a unique improvement over conventional electronics systems [3–8].

Supercapacitors, also known as electrochemical capacitors, have attracted great attention as an energy storage device. Supercapacitors have several advantages over batteries such as high power densities, long life cycles and high reversibility. These devices have been used as power sources in many applications for example: portable electronic devices, electric vehicles and

emergency power supplies [9–11]. Supercapacitors can be divided in two common types: electrochemical double layer capacitors (EDLCs) and pseudocapacitors. In EDLCs, the energy storage is based on the formation of separated electric charges at the interface of a porous electrode material and an electrolyte. The charge storage process is non-Faradaic and chemical oxidation–reduction (redox) reactions should not occur. In contrast, pseudocapacitors are based on several faradaic mechanisms, for example underpotential deposition, redox pseudocapacitance and intercalation pseudocapacitance. In underpotential deposition, a single layer of metal ion is deposited onto a different metal surface, for example the deposition of lead onto a gold electrode. In redox pseudocapacitance (as in $\text{RuO}_2 \cdot n\text{H}_2\text{O}$), electrons are transferred between the electrolyte and the electrode through a fast faradaic redox reactions in the charge storage process. Intercalation pseudocapacitance arises from the intercalation of ions into the layers of redox-active electrode materials accompanied by a faradaic charge-transfer without generating phase change [12–14,23]. The manufacturing of supercapacitors can be accomplished by different methods such as inkjet printing and coating methods including the additive manufacturing process that is generally applied in the rapid prototyping industry [11–15].

Recently, there have been great interests in embedding electronic components and electrical interconnections into 3D structures. Palmer [15] presented a 3D printed embedded structure with conductive ink using Direct Printing (DP) which was then expanded by Medina and Lopes [16,17]. In their research, two different 3D printing techniques were integrated, e.g. stereolithography (SL) and a dispensing system. This method was applied to print simple circuits, including a demonstration of simple

* Corresponding author.

E-mail address: anan.tanwilaisiri@brunel.ac.uk (A. Tanwilaisiri).

prototype temperature sensors. For 3D printed energy storage devices, Sun [18] introduced 3D interdigitated microbattery architectures (3D-IMA). For the anode and cathode materials of this 3D-IMA, $\text{Li}_4\text{Ti}_5\text{O}_{12}$ (LTO) and LiFePO_4 (LFP) were applied respectively. Ho [19] also showed a zinc microbattery with an ionic liquid gel electrolyte using direct write dispenser printing. In this work, a developed dispenser printed a microbattery comprising of zinc and manganese dioxide electrodes which sandwich an ionic liquid gel electrolyte. Zhao [20] presented a 3D printed electrode for fabricating interdigitated supercapacitors using a Selective Laser Melting (SLM) method. In this research, pseudo-capacitors were produced using a 3D interdigitated $\text{Ti}_6\text{Al}_4\text{V}$ electrode which is fine metal powder. Zhu [24] reported fabrication of 3D periodic graphene composite aerogel microlattices for supercapacitor using a direct-ink writing technique. In this study, the 3D-printed graphene composite aerogel (3D-GCA) was produced and fabricated as an electrode. Fu [25] introduced graphene oxide-based electrode inks for 3D printed lithium-ion batteries. In this work, highly concentrated graphene oxide (GO) was selected due to its excellent properties, for example a gel-like behavior and a high elastic modulus. The GO-based electrode inks with high viscosity were used to fabricate lithium-ion battery prototypes using extrusion-based 3D printing. In addition, Zhu [26] reviewed 3D printed functional nanomaterials for electrochemical energy storage. In this literature, manufacturing of batteries and supercapacitors using different types of 3D printing methods were reviewed and showed that 3D printing methods enable fabrication of functional nanomaterials with three-dimensional architectures.

Previous research works have presented 3D printing techniques to create 3D printed electronics in several applications but these have not included EDLC supercapacitors. In this paper, we present a new method of combining 3D printing processes to manufacture EDLC supercapacitors with one continuous process and high reproducibility. In this study, a combination system of Fused Deposition Modelling (FDM) and paste extruder was applied for manufacturing a supercapacitor. The FDM technology was used to print the frame for the supercapacitors, and the paste extruder system was used to print current collector layers, electrodes and separator layer with electrolyte. The method described in this paper showed a new approach for manufacturing embedded energy storage devices.

2. Experiment

2.1. Materials

The material used to build the supercapacitor frame in this experiment is polylactic acid (PLA) filament with a diameter of 2.89 mm. Silver conductive paint was used as the current collector material. The materials used for mixing electrode slurry and

electrolyte include activated carbon (AC) (AR grade, $1375 \mu\Omega \text{ cm}$), Sodium carboxymethyl cellulose, CMC ($\text{C}_{28}\text{H}_{30}\text{Na}_8\text{O}_{27}$, MW: 250,000), ethanol ($\geq 99.8\%$, ACS grade), phosphoric acid (H_3PO_4) and PVA (MW 146,000–186,000, $>99\%$ hydrolysed). Preparation of the electrode slurry was achieved by mixing the activated carbon (AC) with CMC solution. The CMC binder solution was mixed with distilled water/ethanol (1:1) solvent at room temperature. The concentration of CMC was fixed at 5 wt% based on total mass of AC and CMC, in which 2 g activated carbon was added to the 50 mL of CMC binder solution. The slurry prepared was stirred for 8 h before the experiment in order to make it homogeneous and suitable for printing. The conductivity of the slurry was about $10^2 \Omega/\text{sq}$. The gel electrolyte was made by dissolving 0.8 mL H_3PO_4 and 1.0 g PVA in 10 mL deionized water. All the materials used in the experiment are low cost, nontoxic and easily available.

2.2. Printing system

Fig. 1 shows the schematic diagram of the combination of the two 3D printing techniques applied in this study, i.e. a paste extrusion system (Discovery extruder) is attached to a FDM printing machine (Ultimaker2). FDM technology offers a simple fabrication process, reliability, safe, low cost of material and accessibility to several different types of thermoplastics. In the FDM printer, thermoplastic filament material from feedstock spool was driven using two rollers and forced out through a small temperature controlled extruder as shown in Fig. 2. Then the filament was transformed to the semi-molten polymer and deposited onto a platform in a layer by layer process. To build the sample, filament was deposited from the extruder that moved in the x-y plane. When each layer was complete, the base platform was lowered in order to deposit the next layer and so on. The temperature of the base platform was set at low temperature, so that the thermoplastic filament quickly hardens.

The paste extrusion system was employed for building the current collector layer, electrode layer and separator with electrolyte layer. The system consists of a stepper motor, a syringe connected with a plastic tube and a nozzle. During the manufacturing process of supercapacitor, the frame was printed using the FDM printer, whereas, the other materials of the supercapacitor were printed by the paste extruder. In order to deposit the paste materials, the syringe was forced by the stepper motor and paste material flowed along the plastic tube to the nozzle. This function was automated and controlled by CURA software. CURA software was used to control the manufacturing process, which is compatible with both FDM and paste extrusion system, to set up all specifications of printing including transforming STL file to g-code. G-code is one of many programming languages used in machine automation, which has also been used in this manufacturing process to control the speed of the stepper

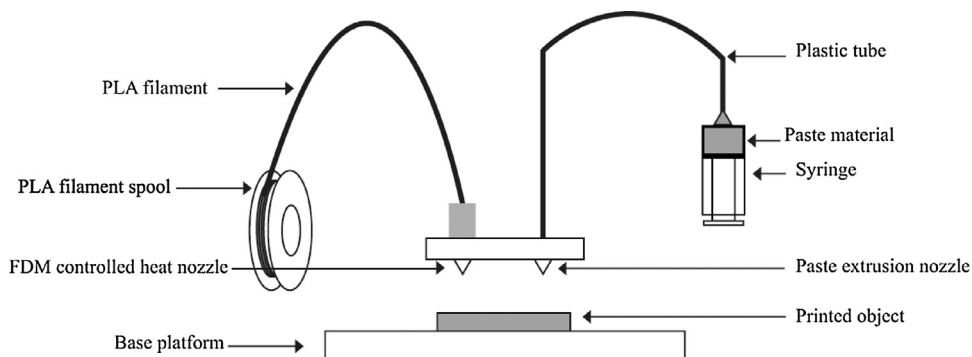


Fig. 1. Schematic of a combination of two 3D printing techniques.

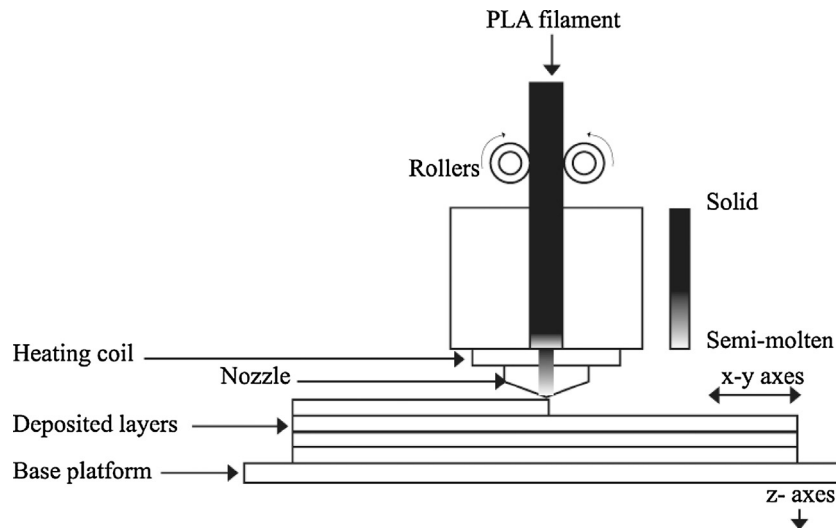


Fig. 2. Schematic diagram of the extrusion and deposition of FDM process.

motor of the paste extrusion system in order for the appropriate amount of the material to be printed. The most distinguished advantage of this manufacturing system is that it utilizes two printing systems at the same time, which can provides the following benefits: 1) different types of materials needed for manufacturing supercapacitors can be applied in the system, 2) the products designed can be fabricated in one continuous process to avoid being moved so a high dimensional accuracy can be achieved, 3) the reproducibility of the product is reliable.

2.3. Design of the supercapacitor

Fig. 3 shows the schematic of the supercapacitor structure. The structure of supercapacitors consists of a current collector and an electrode on each side of the supercapacitor frame with a separator containing the electrolyte in the middle. The frame with thickness of 2.0 mm for the supercapacitor was designed with a hinge, so the supercapacitor printed can be closed up easily to form a complete energy storage module without further assembly. This frame was designed by Solidworks and created by the FDM 3D printing machine. Fig. 4 shows the complete functional supercapacitor modules, which can be extended on to each other to provide more electrical energy as required.

2.4. Manufacture of the supercapacitor

The FDM printing head was used for printing the frame. The speed of printing was adjusted to 50 mm/s. PLA filament material was used in the printing process. In this process, PLA was heated

and extruded through a nozzle with size of 0.4 mm that draws the cross sectional geometry of the part layer by layer. The temperature of the extruder was heated to 220 °C to melt the PLA filament and the platform was kept at 60 °C. After the packaging frame had been printed, the current collector layer was printed on the surface of the frames. The paste extrusion system being connected with FDM printer provided the possibility to print various materials which may not need to be heated, and it enabled the manufacturing process to be continuous without disruption. In this experiment, the extrusion head of the paste extrusion system was set next to the main extrusion without heating the materials. The distance between the extrusion head and substrate was adjusted to approximately 0.5 mm. This type of combined printing system was applied to print three different materials for manufacturing the supercapacitors. Silver conductive paint was printed over area of 3.2 × 3.2 cm on both sides of the frame. The silver paint was printed twice then dried at room temperature before the carbon slurry layer was printed on it in the next step. The drying time used for silver conductive paint was one hour for each layer of the printed silver current collectors. This silver material has been reported in manufacturing of EDLC devices previously [14,30] and in their study, the silver material was used as current collector and presents a satisfactory performance. The electrode material layer (AC slurry) was deposited on top of the silver conductive paint over area of 3.0 × 3.0 cm on each side of the frame. The slurry of the electrode material was printed five times on the same position and dried at room temperature. The drying time used for each time of printed electrode was around 30 min and when the final layer of printed was completed due to the thickness 2 mm, the drying time

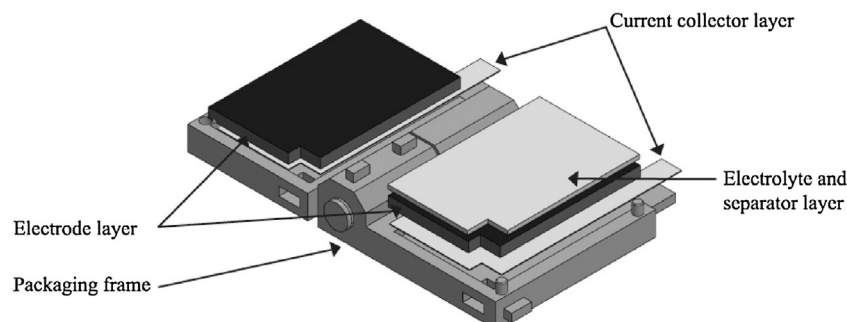


Fig. 3. Schematic of design structure of supercapacitor.

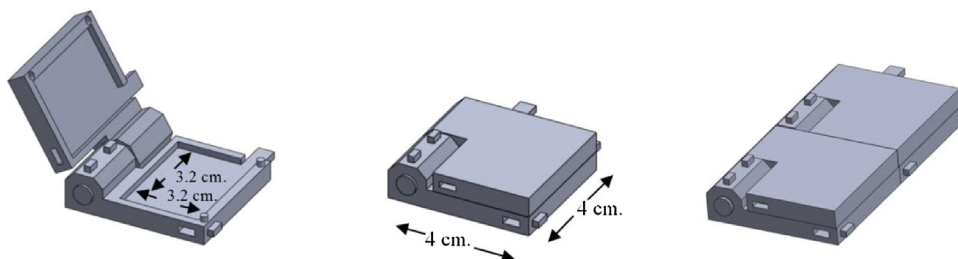


Fig. 4. The frames of the supercapacitor and the extension functionality.

used for the whole printed electrode was around 60 min. Finally, PVA gel electrolyte was printed on top of the AC material in order to build a separator for these supercapacitors, which was only on one side of the 3D frame. The frames were folded over to sandwich the separator, and an assembled electrochemical supercapacitor was completed, as shown in Fig. 5. There was no pressure applied to the EDLC cell due to properties of the gel electrolyte used. This gel electrolyte had excellent film forming and adhesive properties because of the use of PVA. The PVA gel electrolyte not only performed as a separator for the EDLC devices but also behaved as a sealant for the devices. When the EDLC devices were assembled it was certain that both electrodes were in a good contact due to the properties of the gel.

After the initial sample of capacitor (Sample 1) had been made and tested, another three new EDLC samples (Sample 2–4) were manufactured under the same conditions stated above in order to examine the reproducibility of the manufacturing process by the combination of the printing method developed.

3. Methods of testing and characterization

When an electric potential is applied between the two electrodes in EDLC, opposite charges accumulate on the surfaces of the electrodes. The two electrodes in an EDLC are separated by a separator in order to avoid short-circuits and therefore an electric field is created between the two electrodes to complete the function of energy storage. The electrochemical performance of the

supercapacitor printed in this work was studied by cyclic voltammetry (CV) and galvanostatic charge/discharge (GCD) using a Versa-STAT3 electrochemical workstation. These two measurement methods are commonly used to assess quantitative and qualitative data relating to the electrochemical phenomena following to the working electrode.

3.1. Cyclic voltammetry (CV) test

Cyclic voltammetry (CV) is an effective method in the area of electrochemistry. It has been applied to characterize the performance of several electrical energy storage devices, for example batteries and supercapacitors. CV tests are performed by applying a linear potential sweep to the working electrode. A positive (charging) voltage sweeps in a specific voltage range (0–0.8 V) and then reversing (discharging) voltage sweep immediately after the maximum voltage is reached. The electrochemical behavior of the supercapacitor can be assessed from the current response against the applied voltage.

The capacitance, C , of the EDLC can be calculated by the following Eq. (1) [13,14]:

$$C_1 = \frac{Q_{total}}{2\Delta V} \quad (1)$$

Where, Q_{total} is the average integral area of CV curve obtained from the VersaStudio software which represented the total supercapacitor's charge in coulombs. This value was measured from the CV response curve. ΔV is the voltage change between the device's terminals in volts (V)

The specific capacitance is the capacitance per unit mass and can be calculated as follows [22]:

$$Cs_1 = \frac{C}{m} \quad (2)$$

Where Cs_1 is the specific capacitance of the electrode, C is the measured capacitance for the two-electrode cell calculated from Eq. (1), m is total mass of the active material in both electrodes.

3.2. Galvanostatics charge/discharge test

Galvanostatics charge/discharge (GCD) tests can also be used to evaluate the performance of the supercapacitors, which is the most preferred DC (direct current) test. The GCD process is measured by the responsive potential with respect to time unlike CV test, which evaluates data correlating to electrochemical phenomena arising in the electrode material. The measurement is completed in two steps: 1) a constant current charges a supercapacitor first, and then 2) the supercapacitor is discharged in a specific voltage range or charge/discharge time. The capacitance C can be calculated by the following equation:

$$C_2 = \frac{i \cdot \Delta V}{\Delta t} \quad (3)$$

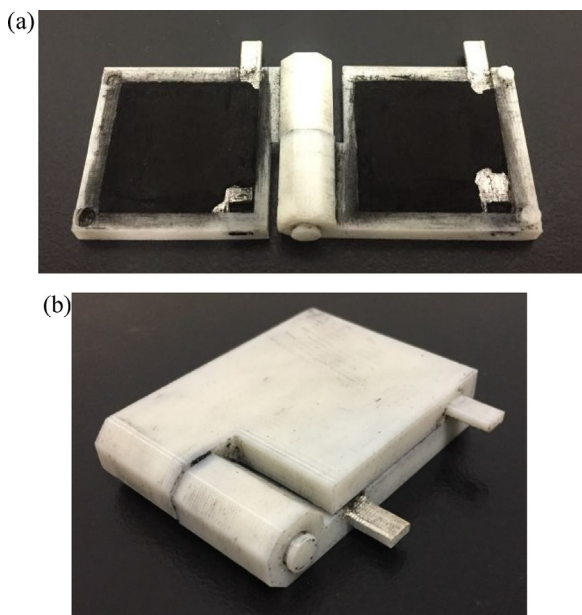


Fig. 5. Printed electrochemical supercapacitor.
(a) Electrode slurry material printed on top of the silver paint.
(b) A complete 3D printed supercapacitor.

Where, i is the discharge current in amperes (mA), Δt is the discharging time (s) and ΔV is the voltage of the discharge excluding iR drop (V) [13,14].

In addition, specific capacitance (C_s) and single-electrode specific capacitance can be calculated from a galvanostatic charge-discharge curve by the following equation:

$$C_{S2} = \frac{i \cdot \Delta t}{m \cdot \Delta V} \quad (4)$$

$$C_{S3} = 4 \cdot C_{S2} \quad (5)$$

Where i is current in amperes (mA), Δt is the charging/discharging time (s), m is the total weight of active materials of two electrodes (g) and ΔV is the voltage of the discharge (V) [31,32].

The energy density and power density of the supercapacitor were calculated as follow [31]:

$$E = \frac{C \cdot \Delta v}{2} \quad (6)$$

$$P = \frac{E}{\Delta t} \quad (7)$$

Where C (mF/cm²) is the specific capacitance of the supercapacitor; ΔV (V) is the applied voltage; Δt (s) is the discharge time. E and P are the corresponding energy density and power density, respectively.

4. Results and discussions

4.1. Characterization of the 3D printed supercapacitor (Sample 1)

CV tests for Sample 1 were carried out and the CV curves were recorded using a potential window range of 0–0.8 V at different scan rates of 0.02 V/s, 0.06 V/s and 0.10 V/s as shown in Fig. 6. The GCD curves recorded (five cycles at a charge current of 15 mA) are shown in Fig. 7.

The shape of the CV curve shows that the device operated as a typical supercapacitor, however, it is not completely rectangular as it would be expected for a perfect supercapacitor. This might be caused by high resistance of electrode material resulting in a deformed rectangular shape. The capacitance calculated using Eq. (1) was 182 mF at the scan rate of 0.02 V/s, and decreased to 65 mF and 32 mF at the scan rates of 0.06 V/s and 0.10 V/s, respectively. It is implied that the change of scan rate affects the performance of the supercapacitor, e.g. the capacitance. The capacitance decreased with the increase of scan rate because the diffusion process of ions is less efficient at the higher scan rate.

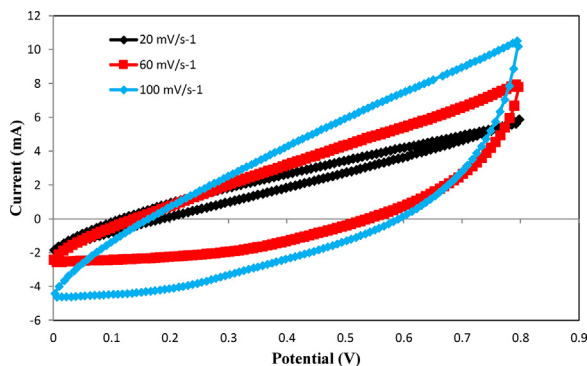


Fig. 6. Cyclic voltammogram curves of the 3D printed supercapacitor sample at different scan rates.

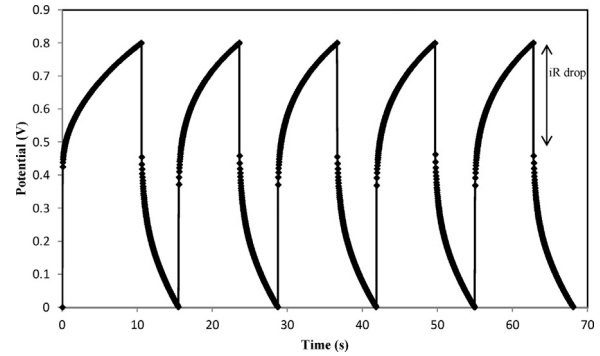


Fig. 7. Galvanostatic charge/discharge curves recorded at a charging current of 15 mA.

Generally, when lower scan rates are applied on the two electrodes of a supercapacitor, the diffused ions from electrolyte have sufficient time to access into the inner porous of the electrode material, providing the supercapacitor with a high electricity capacitance. In contrast, when higher scan rates are employed, the efficiency of ions penetrating into the inner pores of the electrode material is gradually reduced, resulting in a lower electrical capacitance. Similar results of CV curves with different scan rate have been reported previously [27–29]. The highest capacitance of the EDLC (Sample no: 1) printed by the 3D printing process was 182 mF at the scan rate of 0.02 V/s and it was not as high as expected. This is considered to be affected by the high resistance of the AC slurry electrode material due to PVA penetrating into the carbon pores leading to an increase of resistance. The specific capacitance was 193.20 mF/g calculated by Eq. (2).

It can be seen from the charge/discharge curve shown in Fig. 7 that the 3D printed supercapacitor (Sample no: 1) exhibits a stable performance as it can be seen from the similar size of the iR drop for each charge/discharge curve. Five cycles of the charge and discharge curves show an ideal EDLC behavior with a short charge/discharge period of less than 6 s. The capacitance calculated using Eq. (3) from GCD was 224.59 mF, which is slightly different compared to total capacitance obtained from CV curve measured at 0.02 V/s. The different capacitance calculated from these two methods could be due to the time-scales applied in measurement. The time-scales in CV test can be defined using the scan rate and potential window. On the other hand, the GCD tests apply a specific charge/discharge current and a potential window. The total experiment time is a result of the calculated capacitance. The specific capacitance of the printed supercapacitor sample calculated using Eq. (4) from GCD curve was 238.42 mF/g, which was based on the total mass of electrode materials.

In addition, electrochemical impedance spectroscopy (EIS) is a method providing a further study insight of the electrical characteristics of a supercapacitor and can also be applied to the measure and calculation of the equivalent series resistance (ESR). The ESR can be used to determine the resistance of cell components such as contact resistance between current collectors and electrodes and electrolyte resistance. In this method, an electrochemical supercapacitor sample is tested using a small alternating current (AC) over a different range of frequencies (0.01 Hz–1 MHz). The result of measurement derives from changes in current caused by the impedance of the sample and is used to draw on a Nyquist plot which charts imaginary resistance (Z'') against real resistance (Z'). The ESR corresponds to the intersection of the impedance curve at the x-axis in the Nyquist plot [21,22]. Fig. 8 shows a typical Nyquist plot of a 3D printed EDLC at high frequencies from 100 kHz down to 0.01 Hz and the ESR is about 38 Ω . In this study, there is no semicircle shape in the higher

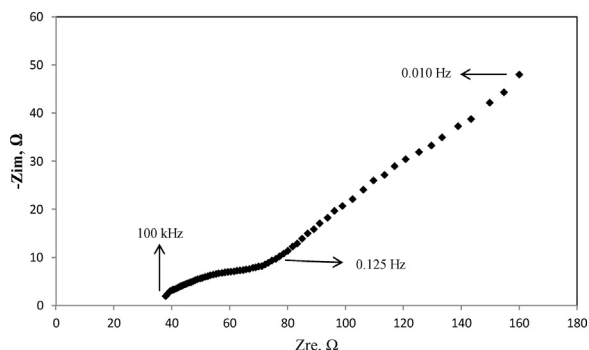


Fig. 8. A typical Nyquist impedance plot of a 3D printed supercapacitor.

frequency range because contact resistance and the charge transfer resistance were low. At intermediate frequencies, some ion diffusion behavior of the electrolyte inside the electrode was seen as the inclined line. At lower frequencies, the device with aqueous acid electrolyte exhibited characteristics of a high internal resistance.

Table 1 shows electrical performance of the 3D printed EDLC. The single-electrode specific capacitance of the device calculated using Eq. (5) was 953.68 mF/g. The energy density was 76.26 mWg⁻¹ with a corresponding power density of 95.36 mWg⁻¹. The 3D printed EDLC showed this limited electrical performance because of high internal resistance. The high internal resistance was probably due to the thickness of the electrode and poor penetration of PVA gel electrolyte and also corrosion of the current collector. The electrode material was prepared using AC and CMC without H₃PO₄ and fabricated with 2 mm thickness. This might have caused a low capacitance because not all pores of the thick carbon electrode were filled with the electrolyte solution. In addition, the PVA gel electrolyte (as separator of the device) that penetrated into the electrode and might obstruct the pores of the carbon electrode may have resulted in inactive areas of the electrode. As mentioned above, both electrode materials have been penetrated by the gel electrolyte. This might have destroyed some area of the silver current collector which would increase the resistance and decrease the capacitance. These three factors significantly influenced the high internal resistance of the device and are reasoned to decrease the capacitance of the device.

Compared to other methods for manufacturing EDLC, 3D printing techniques provided a possible way to create a supercapacitor frame in different sizes and shapes, and paste extrusion system offered a wide range of materials that can be applied to deposit through the system. As mentioned above, integration of the two 3D printing methods encouraged one continuous fabrication process without any movement of sample, potentially giving a high dimensional accuracy of sample. However, the limitation of this method was the lack of a uniform AC printed electrode. The electrode slurry had a low viscosity which resulted in an uneven surface. The properties of the slurry could be improved in the future. In addition, the fabrication technique needs to be carefully controlled to provide consistency.

Table 1
Electrical performance of the 3D printed EDLC (Sample no:1).

Sample	Total mass (mg)	Mass loading (mg/cm ²)	C1 (mF)	Cs1 (mF/g)	C2 (mF)	Cs2 (mF/g)	Energy density (mWs/g)	Power density (mW/g)
no:1	942	45.99	182	193.20	224.59	238.42	76.29	95.36

4.2. Reproducibility of the manufacturing process

After the initial manufacturing and testing, another three new EDLCs (Samples no: 2, 3, and 4) were manufactured under the same conditions as Sample 1 and characterized by CV tests. The CV and GCD curves of the four samples are shown in Figs. 9 and 10. It can be seen that the areas of the CV and GCD curves measured are all similar and the capacitances, and specific capacitances calculated from the CV and GCD curves are only slightly different, as shown in Table 2. The average capacitance and specific capacitance calculated from CV curves for the three new supercapacitors are about 174 mF, and 183.94 mF/g respectively. In addition, the average capacitance and specific capacitance

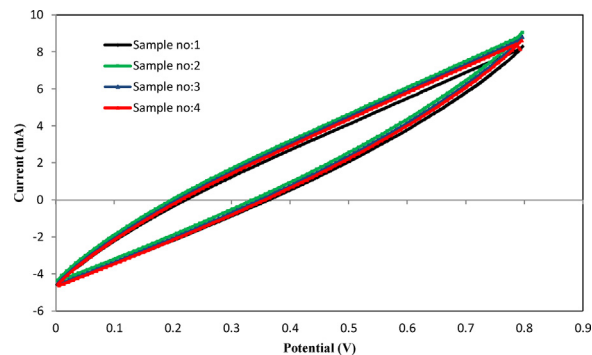


Fig. 9. CV curves of the four EDLC samples at the scan rate of 0.02 V/s.

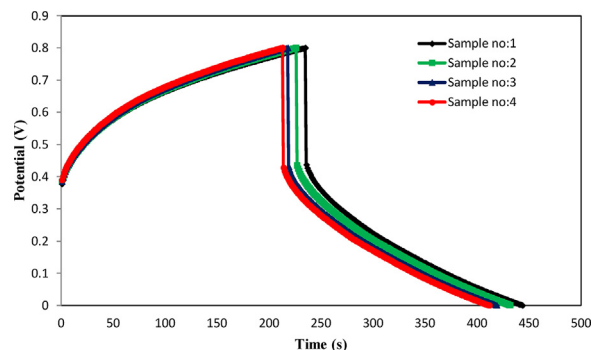


Fig. 10. Galvanostatic charge/discharge curves recorded of the four EDLC samples at a charging current of 15 mA.

Table 2
Capacitance and specific capacitance of four EDLC samples manufactured under the same condition.

Sample	Calculated from CV		Calculated from GCD	
	C1, (mF)	Cs1, (mF/g)	C2, (mF)	Cs2, (mF/g)
no:1	182	193.20	224.59	238.42
no:2	177	189.10	218.02	232.93
no:3	168	171.77	209.43	214.15
no:4	169	181.72	208.77	224.48
Average value	174	183.94	215.20	227.50
Standard deviation (%)	4.93	8.69	5.16	9.40

calculated from GCD curves for the three new supercapacitors are about 215.20 mF, and 227.50 mF/g respectively. Both capacitance and specific capacitance calculated from CV and GCD curves are about 94% and 95% of Sample 1. Standard deviations of all experimental data results are also less than 10%. These results demonstrate that the manufacturing process developed in this study for printing the EDLCs illustrated above has a good reproducibility.

5. Conclusions

The supercapacitors printed using the 3D printer were successfully manufactured and characterized in this study. The combination of the two 3D printing technologies, i.e. a FDM system plus a paste extrusion system to print different materials, has been developed and demonstrated to be a new manufacturing method to fabricate a geometrically complex shape of electrochemical double layer capacitor. The manufacturing process showed a good reproducibility. Nevertheless, the structure of the EDLCs could be optimized in order to avoid the high internal resistance of the EDLCs electrode. In addition, a uniform AC electrode produced by more accurate and consistent control of the manufacturing process may improve the electrical performance of the EDLCs.

References

- [1] S.H. Huang, P. Liu, A. Mokasdar, L. Hou, Additive manufacturing and its societal impact: a literature review, *Int. J. Adv. Manuf. Technol.* 67 (5–8) (2013) 1191–1203.
- [2] M. Vaezi, H. Seitz, S. Yang, A review on 3D micro-additive manufacturing technologies, *Int. J. Adv. Manuf. Technol.* 67 (5–8) (2013) 1721–1754.
- [3] J. Czyżewski, P. Burzyński, K. Gawel, J. Meisner, Rapid prototyping of electrically conductive components using 3D printing technology, *J. Mater. Process. Technol.* 209 (12–13) (2009) 5281–5285.
- [4] D. Espalin, D.W. Muse, E. MacDonald, R.B. Wicker, 3D Printing multifunctionality: structures with electronics, *Int. J. Adv. Manuf. Technol.* 72 (5–8) (2014) 963–978.
- [5] S.J. Leigh, R.J. Bradley, C.P. Purssell, D.R. Billson, D.A. Hutchins, A simple, low-cost conductive composite material for 3D printing of electronic sensors, *PLoS One* 7 (11) (2012) e49365.
- [6] S. Ready, F. Endicott, G.L. Whiting, T.N. Ng, E.M. Chow, J. Lu, '3D printed electronics', NIP & digital fabrication conference, Soc. Imaging Sci. Technol. (2013) 9–12.
- [7] E. Aguilera, J. Ramos, D. Espalin, F. Cedillos, D. Muse, R. Wicker, E. MacDonald, 3D Printing of Electro Mechanical Systems, (2017) .
- [8] J. Sarik, A. Butler, J. Scott, S. Hodges, N. Villar, Combining 3D Printing and Printable Electronics, (2012) .
- [9] R. Kötz, M. Carlen, Principles and applications of electrochemical capacitors, *Electrochim. Acta* 45 (15) (2000) 2483–2498.
- [10] D. Qu, H. Shi, Studies of activated carbons used in double-layer capacitors, *J. Power Sources* 74 (1) (1998) 99–107.
- [11] M. Vangari, T. Pryor, L. Jiang, Supercapacitors: review of materials and fabrication methods, *J. Energy Eng.* 139 (2) (2012) 72–79.
- [12] V. Conédéra, F. Mesnilgrete, M. Brunet, N. Fabre, Fabrication of activated carbon electrodes by inkjet deposition, *Quantum, Nano and Micro Technologies*, 2009 ICQNM'09, Third International Conference on IEEE 157 (2009).
- [13] R. Zhang, Y. Xu, D. Harrison, J. Fyson, F. Qiu, D. Southee, Flexible strip supercapacitors for future energy storage, *Int. J. Autom. Comput.* 12 (1) (2015) 43–49.
- [14] R. Zhang, Y. Xu, D. Harrison, J. Fyson, D. Southee, A. Tanwilaisiri, Fabrication and characterisation of energy storage fibres, *Automation and Computing (ICAC) 2014 20th International Conference on*, IEEE (2014) 228–230.
- [15] J. Palmer, P. Yang, D. Davis, B. Chavez, P. Gallegos, R. Wicker, F. Medina, Rapid prototyping of high density circuitry, *Proc. Rapid Prototyping & Manufacturing 2004 Conference Proceedings 2004* (2004) 10–13.
- [16] F. Medina, A. Lopes, A. Inamdar, R. Hennessey, J. Palmer, B. Chavez, D. Davis, P. Gallegos, R. Wicker, Hybrid manufacturing: integrating direct-write and stereolithography, *Proceedings of the 2005 Solid Freeform Fabrication, Journal of Manufacturing Science and Engineering* (2005).
- [17] A.J. Lopes, E. Macdonald, R.B. Wicker, Integrating stereolithography and direct print technologies for 3D structural electronics fabrication, *Rapid Prototyping J.* 18 (2) (2012) 129–143.
- [18] K. Sun, T. Wei, B.Y. Ahn, J.Y. Seo, S.J. Dillon, J.A. Lewis, 3D printing of interdigitated Li-ion microbattery architectures, *Adv. Mater.* 25 (33) (2013) 4539–4543.
- [19] C.C. Ho, J.W. Evans, P.K. Wright, Direct write dispenser printing of a zinc microbattery with an ionic liquid gel electrolyte, *J. Micromech. Microeng.* 20 (10) (2010) p104009.
- [20] C. Zhao, C. Wang, R. Gorkin Iii, S. Beirne, K. Shu, G.G. Wallace, Three dimensional (3D) printed electrodes for interdigitated supercapacitors, *Electrochem. Commun.* 41 (2014) 20–23.
- [21] M.S. Halper, J.C. Ellenbogen, Supercapacitors: a brief overview, *MITRE Nanosyst. Group* (2006).
- [22] B.K. Kim, S. SY, A. YU, J. Zhang, Electrochemical supercapacitors for energy storage and conversion, *Handb. Clean Energy Syst.* (2015).
- [23] V. Augustyn, P. Simon, B. Dunn, Pseudocapacitive oxide materials for high-rate electrochemical energy storage, *Energy Environ. Sci.* 7 (5) (2014) 1597–1614.
- [24] C. Zhu, T. Liu, F. Qian, T.Y. Han, E.B. Duoss, J.D. Kuntz, C.M. Spadaccini, M.A. Worsley, Y. Li, Supercapacitors based on three-dimensional hierarchical graphene aerogels with periodic macropores, *Nano Lett.* 16 (6) (2016) 3448–3456.
- [25] K. Fu, Y. Wang, C. Yan, Y. Yao, Y. Chen, J. Dai, S. Lacey, Y. Wang, J. Wan, T. Li, Graphene oxide-based electrode inks for 3D-printed lithium-ion batteries, *Adv. Mater.* 28 (13) (2016) 2587–2594.
- [26] C. Zhu, T. Liu, F. Qian, W. Chen, S. Chandrasekaran, B. Yao, Y. Song, E.B. Duoss, J. D. Kuntz, C.M. Spadaccini, 3D printed functional nanomaterials for electrochemical energy storage, *Nano Today* (2017).
- [27] A.M. Obeidat, M.A. Gharaibeh, M. Obaidat, Solid-state supercapacitors with ionic liquid gel polymer electrolyte and polypyrrole electrodes for electrical energy storage, *J. Energy Storage* 13 (2017) 123–128.
- [28] G. Wang, Y. Zhang, F. Zhou, Z. Sun, F. Huang, Y. Yu, L. Chen, M. Pan, Simple and fast synthesis of polyaniline nanofibers/carbon paper composites as supercapacitor electrodes, *J. Energy Storage* 7 (2016) 99–103.
- [29] Z. Tehrani, D. Thomas, T. Korochkina, C. Phillips, D. Lupo, S. Lehtimäki, J. O'mahony, D. Gethin, Large-area printed supercapacitor technology for low-cost domestic green energy storage, *Energy* 118 (2017) 1313–1321.
- [30] M.D. Stoller, R.S. Ruoff, Best practice methods for determining an electrode material's performance for ultracapacitors, *Energy Environ. Sci.* 3 (9) (2010) 1294–1301.
- [31] M. Li, M. Zhou, Z.Q. Wen, Y.X. Zhang, Flower-like NiFe layered double hydroxides coated MnO₂ for high-performance flexible supercapacitors, *J. Energy Storage* (2017).
- [32] H. Yu, Q. Tang, J. Wu, Y. Lin, L. Fan, M. Huang, J. Lin, Y. Li, F. Yu, Using eggshell membrane as a separator in supercapacitor, *J. Power Sources* 206 (2012) 463–468.